PHYSICAL REVIEW B **82**, 060102(R) (2010)

Unusual compression behavior of TiO_2 polymorphs from first principles

Xiang-Feng Zhou (周向锋),[1] Xiao Dong (董校),[1] Guang-Rui Qian (钱广锐),[2] Lixin Zhang (张立新),[1] Yonjun Tian (田永君),[3] and Hui-Tian Wang (王慧田)[1,2,*]

[1]*School of Physics and Key Laboratory of Weak-Light Nonlinear Photonics, Nankai University, Tianjin 300071, China*

[2]*National Laboratory of Solid State Microstructures, Nanjing University, Nanjing 210093, China*

[3]*State Key Laboratory of Metastable Materials Science and Technology, Yanshan University, Qinhuangdao 066004, China*

(Received 1 July 2010; published 12 August 2010)

The physical mechanisms behind the reduction in the bulk modulus of a high-pressure cubic TiO_2 phase are revealed by first-principles calculations. An unusual and abrupt change occurs in the dependence of energy on pressure at 43 GPa, indicating a pressure-induced phase transition from columbite TiO_2 to a modified fluorite TiO_2 with a *Pca*21 symmetry. Oxygen atom displacement in *Pca*21 TiO_2 unexpectedly reduces the bulk modulus by 34% relative to fluorite TiO_2. This discovering provides a direct evidence for understanding the compressive properties of such groups of homologous materials.

DOI: 10.1103/PhysRevB.82.060102 PACS number(s): 61.50.Ks, 61.05.cp, 61.50.Ah, 62.20.−x

Titanium dioxide (TiO_2) has rich phase diagrams, namely, the rutile (*P*42/*mnm*), anatase (*I*41/*amd*), brookite (*Pbca*), columbite (*Pbcn*), baddeleyite (*P*21/*c*), and cotunnite (*Pnma*) phases.[1–6] Due to its versatile physical and chemical properties, TiO_2 is extensively used in many industrial applications, such as high efficiency solar cells, photocatalysis, dynamic random access memory modules, and superhard materials.[7–12] The rutile and anatase phases of TiO_2 are abundant in nature.[13,14] Since the phase sequence of TiO_2 is very similar to that of other bulk materials, such as ZrO_2 and HfO_2, it is highly expected to transform into its cubic polymorphs under pressure.[15] Modified cubic fluorite-structured RuO_2, SnO_2, and PbO_2 that possess a $Pa\bar{3}$ symmetry, have been successfully synthesized.[16] In particular, RuO_2 is considered to be a potential ultrahard material because of its measured Knoop hardness (~20 GPa) and bulk modulus (399 GPa), which is only 10% less than that of sintered diamonds.[17] Moreover, synthesized cotunnite TiO_2 has an extremely high bulk modulus of 431 GPa and is considered as the hardest oxide to date.[1] After the synthesis of cotunnite TiO_2, scientists expected to synthesize cubic TiO_2 because it showed potential for use as a solar cell or ultrahard material. Ultimately, the highly anticipated cubic TiO_2 was successfully synthesized by heating anatase TiO_2 between 1900 and 2100 K in diamond-anvil cells under a pressure of 48 GPa.[18] Some ambiguities, however, remained both in experiment and in theory. For instance, the theoretical bulk modulus calculated for cubic TiO_2 in the pyrite and fluorite phases was significantly larger than that obtained during the experiments. Kim *et al.*[13] showed that pyrite TiO_2 is unstable because of the presence of imaginary frequencies in the phonon spectra throughout the entire pressure range, whereas fluorite TiO_2 is stable because of the absence of these imaginary frequencies under pressure. Swamy and Muddle[19] reported that pyrite TiO_2 has theoretical properties closer to the experimental values because it has a relatively lower bulk modulus. In terms of mechanical properties, however, Liang *et al.*[20] found a minor difference between the fluorite and pyrite phases. At the present stage, there is no theory of the cubic phase of TiO_2, and that although there is some disagreement between existing calculations on candidate phases fluorite and pyrite, both phases appear to be inadequate to explain the high-pressure cubic phase.[18–20] Consequently, even though many efforts have been made to elucidate its properties, some features of cubic TiO_2 remain questionable.

In this work, first-principles calculations are performed using the projector augmented wave method implemented in the *ab initio* total energy and molecular-dynamics program, VASP.[21] We employ a generalized gradient approximation (GGA) given by Perdew-Wang (PW91) (Ref. 22) for the exchange-correlation functional and used a cut-off energy of 500 eV and a Monkhorst-Pack Brillouin-zone sampling grid spacing of 0.5 $Å^{-1}$. During the geometry optimization process, no symmetry and no restrictions are constrained for both the unit cell and the atomic positions. A residual minimization scheme and direct inversions in the iterative subspace are employed. Structural relaxation is prevented until the total energy is less than 10^{-5} eV and the force is less than 10^{-2} eV/Å. The mechanical stability is determined by calculating the phonon-dispersion curves at various pressures using density-functional perturbation theory as implemented in the ESPRESSO package.[23] The GGA-PW91 parametrization, Vanderbilt-type ultrasoft potentials with a cut-off energy of 60 Ry for the wave functions, and a $3\times3\times3$ *q*-point mesh were used to do phonon calculation. To get accurate phonon dispersion of TiO_2 polymorphs, we tested these parameters for rutile TiO_2 at ambient pressure successfully. Powder x-ray diffraction (XRD) patterns are simulated by the REFLEX software.[24]

We begin from the columbite structure and impose hydrostatic pressure on it. As the pressure increases from ambient conditions, we obtain a series of optimized configurations after relaxing the structure under predefined pressure points. The calculated pressure dependency of energy exhibits an unusual and abrupt change at a pressure of 43 GPa [see Fig. 1(a)], suggesting the occurrence of direct structural transition and the appearance of a different phase. By analyzing its symmetry, this different phase is determined to be a modified fluorite structure.

Figure 2 shows the snapshots of the structures along the [010] direction of a $2\times2\times2$ columbite TiO_2 supercell at a transition pressure of 43 GPa. Figures 2(a) and 2(c) show the

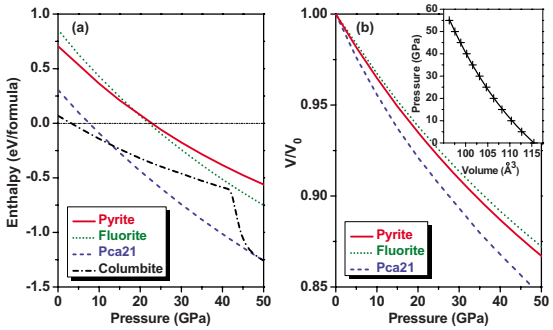

FIG. 1. (Color online) (a) Enthalpies of the pyrite, fluorite, columbite, and *Pca*21 TiO_2 within the pressure range from 0 to 50 GPa. The enthalpy difference is based on that of anatase TiO_2. (b) The pressure-volume relations of the pyrite, fluorite, and *Pca*21 TiO_2. The inset in (b) shows the fitting of the third-order Birch-Murnaghan equation of state for *Pca*21 TiO_2.

initial and the final structure, respectively. For comparison, the fluorite structure is also shown in Fig. 2(d). Clearly, the O atoms undergo large displacements, and the Ti atoms exhibit smaller ones [Figs. 2(a)–2(c)]. As shown in Fig. 2(a), four nearest-neighbor Ti atoms exhibit a near rhombic motif in the starting columbite phase. In contrast, as shown in Fig. 2(c), four nearest-neighbor Ti atoms form a square motif. The O atom in these figures exhibits significant deviation from that in fluorite TiO_2 in Fig. 2(d). Therefore, we became interested in the final structure of TiO_2 and the factors that influence the mechanical properties of the high-pressure phase of cubic TiO_2. The modified fluorite TiO_2 with a tolerance of 0.5 Å has a $Fm\bar{3}m$ symmetry, which is the same as that of the fluorite TiO_2. When the tolerances are 0.1, 0.01, and 0.001 Å, however, the TiO_2 structure is not fluorite; rather, the resulting structures have $P42/nmc$, $Aba2$, and *Pca*21 symmetries. This is determined using *find symmetry* technology.[25] The multifold symmetries of the modified fluorite TiO_2 originate from the uncertainty of the O atom positions. This is responsible for the relatively unstable bonding in the modified fluorite TiO_2 compared with the fluorite TiO_2.

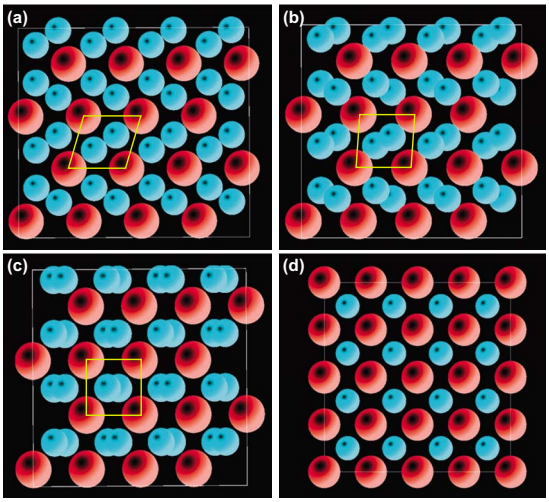

FIG. 2. (Color online) Projections along the [010] direction of a $2\times2\times2$ columbite TiO_2 supercell at 43 GPa. The O and Ti atoms are represented by small and large circles, respectively. (a), (b), and (c) show snapshots of the initial, intermediate, and final stages. (d) shows the fluorite TiO_2 for comparison.

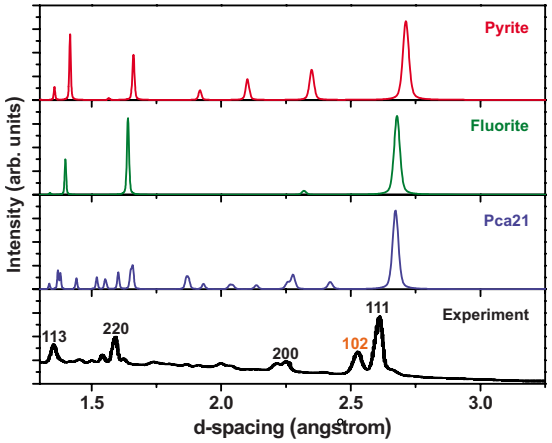

FIG. 3. (Color online) Simulated XRD patterns of the pyrite, fluorite, and *Pca*21 structures at 0.6996 Å and 43 GPa in comparison with the experimental results at 48 GPa. The distinct 102 peak reflects the structure of cotunnite (O II).

To explore the influence of the O atom displacements, we simulated the XRD patterns of *Pca*21 TiO_2, fluorite TiO_2, and pyrite TiO_2 and compared them with the experimental data. Mattesini *et al.*[18] claimed that the fluorite and distorted fluorite phases ($Pa\bar{3}$) cannot be unambiguously distinguished because some weak XRD peaks are screened by the XRD peaks of the cotunnite phase. Our simulation results in Fig. 3 clearly show that the differences in the O positions of pyrite, fluorite, and *Pca*21 phases significantly influence both the positions and relative intensities of the peaks in the XRD patterns. The calculated displacements of the O atoms in the *Pca*21 TiO_2 phase match the experimental results more closely than the other two phases.[18] In particular, the intensity ratios of the 220 peak to the 111 peak are 57% for the pyrite phase, 99% for the fluorite phase, and 33% for the *Pca*21 phase, and its experimental value is 45%. The intensity ratios of the 113 peak to 111 peak are 46% for the pyrite phase, 84% for the fluorite phase, and 24% for the *Pca*21 phase, and its experimental value is 31%. The residual weak peaks, including the 200 peak, also more closely match the experimental data. Consequently, the *Pca*21 TiO_2 phase has the closest match to the experimental data.

The lattice parameters of the *Pca*21 phase are determined and the enthalpies of different phases are compared under various pressures. The results shown in Fig. 1(a) indicate that the *Pca*21 phase has a much lower enthalpy than the other structures within the pressure range. The lattice parameters of the *Pca*21 TiO_2 under 43 GPa are $a=4.84$ Å, $b=4.51$ Å, and $c=4.55$ Å. In the *Pca*21 TiO_2 phase, all identical Ti atoms occupy the 4*a* (0.5428, 0.7265, 0.2112) sites, and all nonidentical O atoms occupy the 4*a* (0.2477, 0.5629, 0.4608) and 4*a* (0.3893, 0.0933, 0.2989) sites. The hypothesis that *Pca*21 TiO_2 could revert directly to the columbite phase under decompression to −1 GPa is also validated in this work.[26] The transition pressure (43 GPa) from the

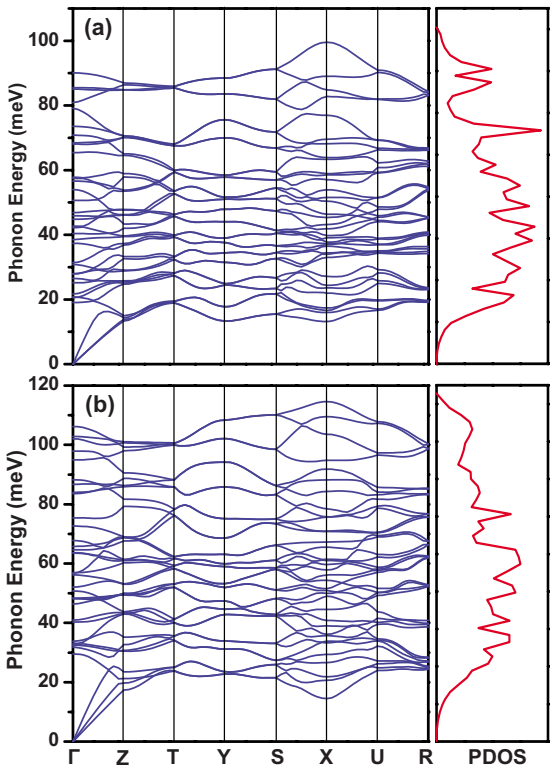

FIG. 4. (Color online) Phonon dispersion curves and phonon density of states for *Pca*21 TiO_2 at (a) zero pressure and (b) 50 GPa.

columbite to the *Pca*21 TiO_2, predicted by the *ab initio* calculations during the compression, has a difference of 5 GPa from the experimental value (48 GPa).[18] The transition pressure (−1 GPa) from the *Pca*21 TiO_2 to the columbite TiO_2, predicted by the *ab initio* calculation during the decompression, has a difference of 10 GPa from the experimental value (9 GPa).[18] The difference in transition pressures between the theoretical and experimental values may be attributed to the fact that the *ab initio* calculations are performed in the ground state at zero temperature. The phonon dispersions of *Pca*21 TiO_2 are also calculated from 0 to 50 GPa. The results indicate that the *Pca*21 phase is stable at least in this pressure range because no imaginary frequencies in the phonon spectra curves (as shown in Fig. 4).

Even when the same pressure-transmitting medium (NaCl) is used to measure the bulk moduli, the measured values show discrepancies of about 20% for the columbite, 40% for the baddeleyite, 29% for the orthorhombic I, and 32% for the cotunnite phases.[27] It is thus unsurprising that discrepancies exist between the theoretical and experimental bulk moduli obtained for the system under study. The underlying physics behind such a discrepancy is not clear at present, considering that many possible factors, including the quality of different samples and the different methods employed for measuring bulk modulus, exist. In addition, working with data such that they fit the third-order Birch-Murnaghan equation of state may yield discrepancies.[28] The third-order Birch-Murnaghan equation of state may be written as

TABLE I. Calculated equilibrium volume V_0 (Å^3), bulk modulus B_0 (GPa), and its pressure derivative B' at zero pressure, compared with other available data for the TiO_2 polymorphs.

Phase	Method	V_0	B_0	B'	Reference
Fluorite	VASP-GGA	112.70	277	4.07	This work
	CRYSTAL-GGA	112.75	395	1.75	19
	B3LYP	112.13	390	2.06	19
	BSTATE-GGA	112.11	272	4.66	20
	VASP-LDA	107.08	309	4.46	20
Pyrite	VASP-GGA	117.73	258	4.27	This work
	CRYSTAL-GGA	118.62	220	4.86	19
	B3LYP	117.26	258	4.35	19
	BSTATE-GGA	116.65	272	4.58	20
	VASP-LDA	112.10	298	4.15	20
*Pca*21	VASP-GGA	115.46	207	4.24	This work
	Experiment	115.50	202	1.30	18
Rutile	VASP-GGA	64.34	221	4.80	This work
	CRYSTAL-GGA	63.78	215	5.35	19
	B3LYP	63.42	224	5.64	19
	Experiment	62.44	211	6.76	29

$$P = \frac{3B_0}{2}\left[\left(\frac{V_0}{V}\right)^{7/3} - \left(\frac{V_0}{V}\right)^{5/3}\right] \times\left\{1 - \frac{3(4-B')}{4}\left[\left(\frac{V_0}{V}\right)^{2/3} - 1\right]\right\}, \quad (1)$$

where V and V_0 are the volume at pressure P and the equilibrium volume at ambient pressure, respectively; and B_0 and B' are the bulk modulus at ambient pressure and its pressure derivative, respectively. The uncertainty of the positions of the O atoms gives rise to large discrepancies in the bulk modules of the TiO_2 polymorphs. The reported pressure derivative B' was ~4.0 in literature.[6,20,27] Using the squared residuals fitting method and choosing B' as the adjustable parameter, Hamane *et al.*[27] found that smaller B' values result in larger B_0 values. The optimal value for cotunnite TiO_2 is $B'=4.25$. Thus, this result is expected to be helpful in determining the same values for the other TiO_2 polymorphs. We get the bulk moduli and the pressure derivative of TiO_2 polymorphs from a fit to Eq. (1) and Table I list our calculated results and compares them with reports in Refs. 18–20 and 29. The table shows that lower B' values result in higher B_0 values. The local-density approximation method leads to overestimated B_0 values for the TiO_2 polymorphs because it underestimates V_0. However, our calculated V_0 (115.5 Å^3) and B_0 (207 GPa) for *Pca*21 TiO_2 are in excellent agreement with the experimental data (115.5 Å^3, 202 ± 5 GPa).[18] In addition, the calculated value of B' (4.24) is consistent with the value of B' (4.25), as predicted in Ref. 27.

The calculated volume–pressure curves of the three possible phases (pyrite, fluorite, and *Pca*21) are shown in the Fig. 1(b). They reveal that fluorite TiO_2 is the most incompressible phase among all the predicted phases while *Pca*21 TiO_2 is more compressible than the fluorite and pyrite TiO_2

phases. Swamy and Muddle[19] indicated that the calculated values of B_0 for the pyrite and fluorite phases were significantly larger than the experimental values because of the coexistence of many possible phases in the synthesized sample.[18] Combined with the simulated XRD patterns and the equation of state, we provide direct evidence from the atomic level that the distortions of the O atoms play a dominant role in defining the compressive property of the sample. For the fluorite phase at the transition pressure of 43 GPa, Ti-O bonds with bond lengths of 2.01 Å have a coordination number of eight. In contrast, for *Pca*21 TiO_2, at the transition pressure of 43 GPa, the Ti-O bonds with average bond lengths of 1.966 Å (bond lengths ranged from 1.86 to 2.07 Å) have a coordination number of seven. Due to the very small volume difference between the fluorite (99.8 $Å^3$) and *Pca*21 (99.5 $Å^3$) TiO_2 phases at 43 GPa, the bonding instability in the *Pca*21 phase leads to a significant degree of bond-length fluctuations, which may decrease the coordination number of the Ti-O bonds. Based on Cohen's empirical formula: $B_0 \propto N_c/d^{3.5}$, where N_c is the coordination number of a chemical bond and d is the bond length,[30] the decrease in the coordination number of the chemical bonds in *Pca*21 TiO_2 with respect to fluorite TiO_2 is one of the reasons for the large reduction in bulk modulus in cubic TiO_2 polymorphs. As such, *Pca*21 TiO_2 is more compressible than the fluorite phase within the pressure range under study [Fig. 1(b)]. The minute distortions of the O atoms dominate the unexpected reduction (~34%) in the bulk modulus at pressures of 277 GPa for the fluorite TiO_2, 207 GPa for the *Pca*21 TiO_2, and 202 GPa for the measured value in high-pressure cubic phases. We believe that this evidence clarifies the ambiguity of the bulk modulus in the high-pressure phases of TiO_2. For example, if there exists a similar modified cotunnite phase, the expected bulk modulus reduction in ~30% with respect to cotunnite TiO_2 (431 GPa) in Ref. 1 is in good agreement with independent experimental values of 312 ± 34 GPa in Ref. 6 and 294 ± 9 GPa in Ref. 27.

In conclusion, using *ab initio* calculations, we showed that an unusual and abrupt change in the energy curve of columbite TiO_2 at ~43 GPa produces modified fluorite TiO_2, a structure that had been theoretically conceived but never confirmed. The modified fluorite TiO_2 showed improved simulated XRD patterns. The modified fluorite TiO_2 could be reversed to the columbite TiO_2 under decompression to about −1 GPa. In particular, tiny distortions of the O atom positions result in an unexpected reduction in bulk modulus of about 34% in its high-pressure cubic phases. All of these are in good agreement with the experimental results.

This work is supported by the National Basic Research Program of China under Grants No. 2006CB921805 and No. 2010CB731605, and the Postdoctoral Fund of China under Grant No. 20090460685.

*htwang@nankai.edu.cn; htwang@nju.edu.cn

[1] L. S. Dubrovinsky *et al.*, Nature (London) **410**, 653 (2001).
[2] S. L. Hwang *et al.*, Science **288**, 321 (2000).
[3] A. E. Goresy *et al.*, Science **293**, 1467 (2001).
[4] N. A. Dubrovinskaia *et al.*, Phys. Rev. Lett. **87**, 275501 (2001).
[5] J. Muscat *et al.*, Phys. Rev. B **65**, 224112 (2002).
[6] Y. Al-Khatatbeh *et al.*, Phys. Rev. B **79**, 134114 (2009).
[7] R. Asahi *et al.*, Science **293**, 269 (2001).
[8] H. G. Yang *et al.*, Nature (London) **453**, 638 (2008).
[9] Y. Gai *et al.*, Phys. Rev. Lett. **102**, 036402 (2009).
[10] M. Mattesini *et al.*, Phys. Rev. B **70**, 115101 (2004).
[11] B. H. Park *et al.*, Appl. Phys. Lett. **80**, 1174 (2002).
[12] V. Swamy *et al.*, Appl. Phys. Lett. **89**, 163118 (2006).
[13] D. Y. Kim *et al.*, Appl. Phys. Lett. **90**, 171903 (2007).
[14] V. Swamy *et al.*, Phys. Rev. Lett. **103**, 075505 (2009).
[15] S. Desgreniers and K. Lagarec, Phys. Rev. B **59**, 8467 (1999).
[16] J. Haines *et al.*, Science **271**, 629 (1996); J. Haines *et al.*, Annu. Rev. Mater. Res. **31**, 1 (2001).
[17] J. M. Léger *et al.*, Appl. Phys. Lett. **79**, 2169 (2001).
[18] M. Mattesini *et al.*, Phys. Rev. B **70**, 212101 (2004).
[19] V. Swamy and B. C. Muddle, Phys. Rev. Lett. **98**, 035502 (2007).
[20] Y. Liang *et al.*, Phys. Rev. B **77**, 094126 (2008).
[21] Software VASP, Vienna, 1999, www.materialsdesign.com; G. Kresse and J. Furthmüller, Phys. Rev. B **54**, 11169 (1996); Comput. Mater. Sci. **6**, 15 (1996).
[22] J. P. Perdew *et al.*, Phys. Rev. B **46**, 6671 (1992).
[23] P. Giannozzi *et al.*, J. Phys.: Condens. Matter **21**, 395502 (2009).
[24] X. F. Zhou *et al.*, Phys. Rev. B **76**, 100101(R) (2007).
[25] X. F. Zhou *et al.*, Phys. Rev. B **79**, 212102 (2009).
[26] X. Zhou *et al.*, arXiv:1004.4321 (unpublished).
[27] D. Nishio-Hamane *et al.*, Phys. Chem. Miner. **37**, 129 (2010).
[28] F. Birch, J. Geophys. Res. **57**, 227 (1952).
[29] T. Arlt *et al.*, Phys. Rev. B **61**, 14414 (2000).
[30] M. L. Cohen, Science **261**, 307 (1993); Phys. Rev. B **32**, 7988 (1985).